 ICCES, vol.3, no.1, pp.21-27, 2007

# Multiscale Modeling in Property Predictions of Materials

K.G. Wang[1]

## Summary

A framework of applications of multiscale modeling to property prediction of advanced materials will be briefly presented. A methodology will be shown to link micro-scale to the continuum scale, integrating micro-scale modeling of microstructure with the large Thermo-Calc© database. This paradigm is successfully applied to the case of Fe-12Ni-6Mn maraging steel. We predict the mechanical properties of the maraging steel such as hardness. We found that our predictions in hardness is in agreement with experimental data.

## Introduction

Understanding the precise and fundamental manner in which materials structures (nanostructures or microstructures) and their evolution influences properties and service lifetimes of advanced materials profoundly impacts material design, and today materials design plays an increasingly important rôle in many engineering applications. Linking structures to properties and predicting properties of materials, however, cover a multitude of length scales, making the applicable physics often difficult to judge.

Precipitation strengthening remains one of the most effective means for improving ultra-high strength alloys. For example, ultra-high strength steels, such as maraging steels, have been developed over the past 40 years for aircraft, aerospace, and tooling applications. Maraging refers to the aging of martensite, which is obtained easily in these steels at ordinary cooling rates due to their high nickel content [1]. The mechanism thought to be responsible for strengthening is that of second-phase precipitates acting as a dispersion of obstacles to dislocation movement. Mott and Nabarro [2] introduced the concept of dislocations to explain the mechanism of precipitation hardening. Orowan [3] then established the relationship between the applied stress and the extent of dislocation bowing. Kelly and Nicholson [4] reviewed the earlier efforts at formulating models for precipitation hardening. Brown and Ham [5] reviewed the advances made in understanding the mechanisms of precipitation hardening based on dislocation interactions with precipitates. Ardell [6] discussed in detail the progress achieved through the early 1980s with the theory of precipitation hardening, focusing on the statistical nature of dislocation–precipitate interactions and the kinetic mechanisms of precipitation. It is now well known that precipitation kinetics directly affects age hardening phenomena, and the maturity and sophistication of kinetic models describing population dynamics during

[1]Physics and Space Sciences Department, Materials Science and Nanotechnology Institute, Florida Institute of Technology, Melbourne, FL 32901

solid-state precipitation have progressed steadily over time. The first statistical mechanical formulation of the kinetics of precipitate aging, now called LSW theory, was published by Lifshitz and Slyozov [7], for diffusion-limited precipitate growth, and by Wagner [8] for interface-limited growth. These early mean-field formulations are valid only in the limit of a vanishing small volume fraction of precipitates, where essentially one particle interacts with the mean field of its surrounding matrix. The prediction of LSW theory that the cube of the average length scale of particles increases linearly with time was validated by numerous experiments, even in cases where there was a finite volume fraction of the dispersed phase. The most significant limitation within LSW theory is its neglect of any interactions occurring among the particles. In LSW theory, the growth rate of a precipitate particle is given by the linear form

$$\frac{dr}{dt} = \frac{K_{LSW}}{r}\left(\frac{1}{r^{\star}} - \frac{1}{r}\right), \tag{1}$$

where $r$ and $r^{\star}$ are the radius of the particle, and the critical radius of the precipitate population, respectively. $K_{LSW}$ is the kinetic rate constant and is independent of the volume fraction of the precipitates. In real materials, however, the volume fraction of precipitates, $V_V$, is never zero, so that even in dilute dispersions the mean separation between precipitates, is typically less than a few particle diameters, so that interactions normally occur among the individual particles. Our micro-scale modeling of microstructure, diffusion screening theory, for precipitation kinetics [9], by contrast, considers many-body interaction and modifies the dependence of the growth rate of particles in a non-linear form

$$\frac{dr}{dt} = \frac{K_{LSW}}{r}\left(\frac{1}{r^{\star}} - \frac{1}{r}\right)\left(1 + \frac{r}{R_D}\right), \tag{2}$$

where $R_D$ is the diffusion screening length which depends on the volume fraction [9]. Introducing many-body interactions insures that the coarsening rate of precipitates depends on their volume fraction. Moreover, micro-scale modeling of microstructure for precipitation kinetics recently yielded predictions that were in quantitative agreement with experimental kinetic results [9].

In this study, we combine a micro-scale modeling of microstructure with a macro-scale model for precipitation-enhanced hardening. Specifically, we use: (1) Thermo-Calc© coupled to Kaufman's binary alloy data base to obtain equilibrium values of the solubility at different temperatures. These data, in turn, are used to calculate the kinetic coefficients appearing in the theoretical precipitation kinetics during overaging. (2) We use the Ashby–Orowan formulation to develop the relationship among hardness levels, particle size and spacing. We implement the overall methodology by applying it to the ternary alloy Fe-12Ni-6Mn. The organization of this paper is as follows: in section II, we outline briefly the multiscale

modeling. In section III, the analysis, calculations, and main results for the case of alloy Fe-12Ni-6Mn are presented.

## Multiscale Modeling

In the case of non-zero volume fraction of precipitate, the cubed average radius of the particles remains proportional to time, but the proportionality coefficient is different from that indicated in LSW theory. Therefore, three modifications are required regarding LSW theory to extend its validity to the general case of precipitation hardened alloys. First, the Gibbs–Thomson correction $[(1-c_\alpha)/(c_\beta-c_\alpha)]\varepsilon^{-1}$ must be included, particularly when considering the case of precipitates that are intermetallic compound. When $c_\alpha$, the molar volume of the $\theta$-NiMn precipitate phase, is small, Darken's correction factor, $\varepsilon^{-1}$, approaches unity. Second, the amount of solute needed for precipitate growth, $c_\beta - c_\alpha$, must also be included, where $c_\beta$ is the equilibrium concentration of the elements in the new precipitate phase also expressed as a mole fraction. Finally, the effect of volume fraction on coarsening needs to be included by introducing a parameter $K_c(V_V)$, which is a function of $V_V$. After including each of the modifications mentioned above, the growth law Eq.(2) in our micro-scale modeling for a non-zero precipitate volume fraction becomes

$$\langle r(t)\rangle^3 - \langle r(t_0)\rangle^3 = M\frac{D}{R_g T}(t-t_0), \tag{3}$$

where the coefficient

$$M = \frac{8}{9}\sigma c_\alpha V_m^\theta \frac{c_\alpha(1-c_\alpha)}{(c_\beta-c_\alpha)^2}K_c(V_V). \tag{4}$$

The value of $K_c(V_V)$, however, depends on the specifics of the coarsening kinetics. Our micro-scale modeling yield $K_c(V_V) > 1$, which as indicated is a function of the volume fraction, $V_V$. Values of $V_V$ in case of the Fe-12Ni-6Mn alloy considered here fall between $0 \leq V_V \leq 0.15$ depending on the temperature. The micro-scale modeling [9] [10] yields a value for the function $K_c(V_V)$ that may be expressed as

$$K_c(V_V) = 6.4125\left[\frac{2-(1-\sqrt{3V_V})\left(1-\frac{1}{\sqrt{3V_V}}+\sqrt{\frac{1}{3V_V}+\frac{1}{\sqrt{3V_V}}+1}\right)}{[1-\frac{1}{\sqrt{3V_V}}+\sqrt{\frac{1}{3V_V}+\frac{1}{\sqrt{3V_V}}+1}]^3}\right]. \tag{5}$$

Orowan [11] first studied the mechanism of hardening in a matrix containing a dispersion of hard particles using the concept of dislocation bowing. He established a relationship between the applied stress and amount of bowing along the dislocation line, known as Orowan's equation. Ashby [12] added the effects introduced by the statistical distribution of particle spacings in Orowan's equation, and obtained

the so-called Ashby–Orowan equation, namely,

$$\Delta\tau_y = 0.84\frac{1.2Gb}{2\pi\langle L\rangle}\ln\frac{\langle r\rangle}{b}, \tag{6}$$

where $\Delta\tau_y$, $G$, and $b$ are the increase in the shear stress, the shear modulus of the matrix, and the Burgers vector of the dislocation, respectively. $\langle L\rangle$ and $\langle r\rangle$ are the average interparticle spacing, and the average particle radius, respectively, both of which provide key characteristics of the microstructure. Equation (6) is macro-scale modeling assuming that the precipitates are spheres, the relationship between the volume fraction of the precipitates and their average spacing and average radius is given by [13]

$$\langle L\rangle = p\langle r\rangle, \tag{7}$$

where the auxiliary function $p(V_V)$ is

$$p(V_V) = 1.23\sqrt{\frac{2\pi}{3V_V}} - 2\sqrt{\frac{2}{3}}. \tag{8}$$

The Johnson–Mehl–Avrami (JMA) equation [14]-[16] may be used to describe the time dependence of the dispersoid's volume fraction with time at a given temperature as follows,

$$V_V(t) = V_V(0)\left[1 - \exp[-(kt)^m]\right], \tag{9}$$

where $V_V(0), k, m, t$ represent the equilibrium volume fraction of the precipitates, the JMA reaction rate constant, the Avrami index, and the aging time, respectively. The increase in yield stress for maraging steels is proportional to its hardness increase, $\Delta H$. The Taylor factor, $M_T$, [13] derived for isotropic polycrystalline materials relates the increase in the material's yield stress to the increase in the shear stress associated with dislocation bowing. Thus, one finds that $\Delta\sigma_y$,

$$\Delta\sigma_y = M_T\Delta\tau_y = q\Delta H, \tag{10}$$

where $q$ is the conversion constant relating the Vickers hardness to the yield strength. Combining Eqs.(6) through (10) yields a relationship between the hardness increase in a precipitation hardened microstructure and the average precipitate radius,

$$\Delta H = 0.84\left(\frac{1.2GM_T}{2\pi qp}\right)\frac{b}{\langle r\rangle}\ln\frac{\langle r\rangle}{b}. \tag{11}$$

Equation (11) demonstrates the link micro-scale (microstructure) to macro-scale (the mechanical behavior) of a precipitation-hardened material. If the micro-scale quantities such as volume fraction, $V_V$, of the dispersoid phase changes, both the average particle size, $\langle r\rangle$, and the average inter-particle spacing, $\langle L\rangle$ can be calculated from micro-scale modeling, the hardness can also be predicted by Eq.(11) . This is main governing equation for multiscale modeling.

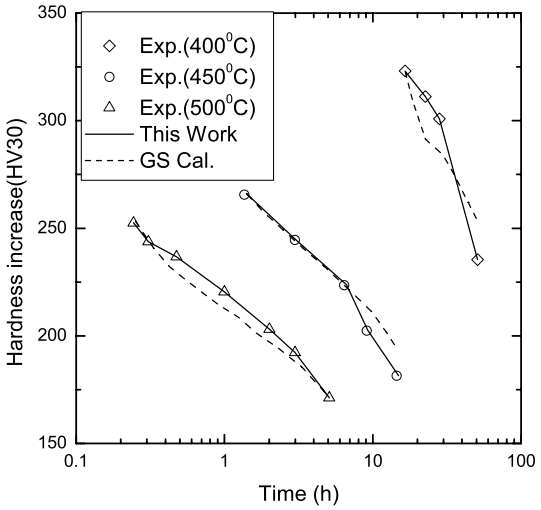


Figure 1: Comparison of hardness calculated from this work to experimental [19] and Guo and Sha's previous calculation [18]. Symbols of unfilled diamond, circle and triangle represent experimental results at temperatures of 400, 450, and 500 °C, respectively. Solid line represents our results, and dashed line represent Guo and Sha' calculation [18].

## Application of Multiscale Modeling to Property Predictions

We apply the multiscale modeling to the alloy, Fe-11.9Ni-5.75Mn (wt.%). The interfacial energy of the NiMn precipitate/matrix interface is estimated to be 750 mJ/m$^2$, which is a reasonable value for an incoherent interface. All other parameters used in these calculations are summarized in [17]. The JMA reaction rate parameter, $k$, in Eq.(9) can be calculated as $k_0 \exp(-Q/RT)$, where $k_0$ and $Q$ are the rate coefficient and its activation energy. Adjustable parameters do not appear in any of microstructure and hardness calculations presented here. Both $c_\alpha$ and $c_\beta$ are the sum of atomic fractions of Ni and Mn present in the matrix and precipitate phases, respectively. Since NiMn only contains Ni and Mn, $c_\beta = 1$ always. The values of $c_\alpha$ at different aging temperatures were calculated using Thermo-Calc© linked to Kaufman's binary alloy database [18]. The values of $c_\alpha$ and the equilibrium amounts of NiMn precipitate at different temperatures are listed in [18]. Note that $c_\alpha$ increases by about 20% as the temperature increases from 400 to 500 C, so it would be inappropriate to consider $c_\alpha$ as constant over this range of aging temperatures. During aging and overaging, the volume fraction of the precipitate, $V_V$, also changes with time, a process which is estimated through Eq.(9). Squires and Wilson [19] measured hardness data for this alloy during overaging. These investigators measured hardness at different overaging times, from 16.5 to 50.9 hr

at 400 C, from 1.4 to 14.5 hr at 450 C, and from 0.244 to 5 hr at 500 C. The quantity $M$ is related to both kinetic and thermodynamic factors. The kinetic factor $K_c(V_V)$ is a complicated function of the volume fraction of precipitates, which can be calculated through Eq.(5). The thermodynamic factor, including $c_\alpha$ and $c_\beta$, is calculated by Thermo-Calc© software. Finally, using Eqs.(11), (3)-(5) one can calculate hardness increase of Fe-12Ni-6Mn. Our prediction in the hardness increase is compared with experimental result and Guo and Sha' calculation in Fig. 1. Fig. 1 shows that our prediction is in good agreement with experimental result and better than Guo and Sha' calculation. In future, we will plan to apply the multiscale modeling to other alloy systems. On the other hand, we will also plan to do multiscale simulations to predict the hardness increase.

## References


1. Rohrbach, K. and Schmidt M. (1990): *Metals Handbook*, 10th Ed., ASM, Materials Park, OH, p. 793.
2. Mott, N. F. and Nabarro, F.R.N. (1968): *Precipitation Hardening*, 1st ed., ed. J.W. Martin, Pergamon Press, Oxford, pp.196-200.
3. Orowan, E. (1968): *Precipitation Hardening*, 1st ed., ed. J.W. Martin, Pergamon Press, Oxford, pp. 201-202.
4. Kelly, A. and Nicholson, R. B. (1968): *Precipitation Hardening*, 1st ed., ed. J.W. Martin, Pergamon Press, Oxford, pp. 208-213.
5. Brown, L.B. and Ham, R.K. (1971): *Strengthening Methods in Crystals*, eds. A. Kelly and R.B. Nicholson, Chapter 2, Elsevier, Amsterdam, pp. 9-135.
6. Ardell, A.J. (1985): "Precipitation hardening," *Metall. Trans. A*, Vol. 16A, P. 2131.
7. Lifshitz, I.M. and Slyozov, V.V. (1961): "The Kinetics of Precipitation from Supersaturated Solid Solution," J. Phys. Chem. Solids **19**, 35.
8. Wagner, C. (1961): "Theorie der Alterrung von Niederschlagen durch Umlosen," Z. Elektrochem. **65**, 581.
9. Wang, K.G., Glicksman,M.E. and Rajan, K. (2004): "Modeling and Simulation for phase coarsening: a comparison with experiment," *Phys. Rev. E*, Vol.69, 061507.
10. Wang, K.G., Glicksman,M.E. and Rajan, K. (2005): "Length Scales in Phase Coarsening: Theory, Simulation, and Experiment," *Computat Mater Sci* Vol.34, PP. 235-253.
11. Orowan, E. (1948): *Internal Stress in Metals and Alloys*, The Institute of Metals, London, p451.

12. Ashby,M.F. (1958): *Oxide Dispersion Strengthening*, Eds. G.S. Ansell, T.D. Cooper, F.V. Lenel, Gordon and Breach, New York, NY, pp.143-205.
13. Martin, J.W. (1998): *Precipitation Hardening*, 2nd Ed., Butterworth-Heinemann, Oxford, pp.58-59, p.81.
14. Johnson and W.A., Mehl, R.F. (1939): *Trans. Am. Inst. Min. Metall. Engrs*, Vol.135, 416.
15. Avrami, M. (1941): *J. Chem. Phys*., Vol. 9, P.177.
16. Burke, J. (1965): *The Kinetics of Phase Transformation in Metals*, Pergamon, Oxford, p.46.
17. Wang, K.G. et al., (2005): "Property Predictions using Microstructural Modeling," *Acta Mater.* Vol.53, PP. 3395-3402.
18. Guo, Z. and Sha, W. (2002): " Quantification of precipitation kinetics and age hardening of Fe-12Ni-6Mn alloy during overaging," *Mater. Sci. Technol.*, Vol. 18, p.529.
19. Squires, D.R. and Wilson, E. A. (1984): "Kinetics of Aging in an Fe-12Ni-6Mn Maraging Alloy" *Metall. Trans. A*, Vol. 15A, P. 1947.